# Passive Acoustic Volume Control

Byung Hoon Cho

9 November 2016

# Table of Contents

# 1 Introduction

Amplifying signals is an easy way to make sounds louder. However, amplifying and attenuating sounds without extra external energy input is much more difficult. This report tests cheap and efficient devices such as lenses which can be used to amplify or attenuate acoustics passively. Uses for these include targeted alarm clocks and reducing noise pollution in areas of high road traffic.

Current research [1][2] in this field is limited to ultrasound frequencies above 20 kHz on a miniature scale (<10 cm). However, for more widespread, practical applications, sounds of frequencies in the audible range for a human (20 Hz - 20 kHz) were used throughout this research. A museum exhibition [3] in Nagoya demonstrates the ability to amplify sounds in this range.

# 2 Design

The idea for this project originates from previous work done as preparation for a problem in the 2016 International Young Physicists' Tournament (`http://www.iypt.org`). The problem was:

> *"Fresnel lenses with concentric rings are widely used in optical applications, however a similar principle can be used to focus acoustic waves. Design and produce an acoustic lens and investigate its properties, such as amplification, as a function of relevant parameters."*

Sounds are transmitted through a medium such as air by longitudinal waves which cause regions of varying pressure. One commonly accepted characteristic of a wave is its ability to diffract: the spreading of waves after passing an obstacle or through a gap (Figure 2.1).

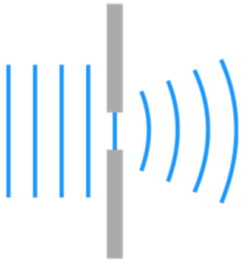

Figure 2.1: Diffraction

The blue lines represent wavefronts moving to the right, obstructed by a grey wall with a gap. The wavefront spreads radially after passing through the gap.

Furthermore, when two or more waves pass through the same point in space at the same time (Figure 2.2a), the displacement of the observed wave is the vector sum of the individual displacements of each of the component waves, and can result in a larger amplitude wave due to constructive interference (Figure 2.2b) or a smaller amplitude wave due to destructive interference.

(a) Two waves represented as transverse waves

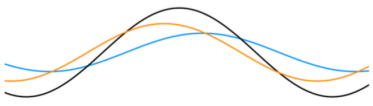

(b) Resultant wave (black) of greater amplitude

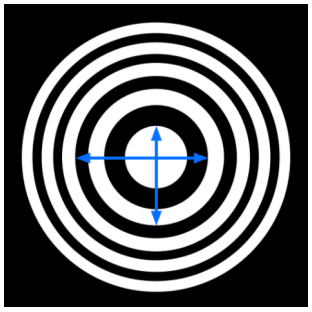

Figure 2.3: Fresnel Zone Plate

Using these two inherent characteristics of acoustic waves, a simple device (Figure 2.3) can be designed to amplify or attenuate sounds passively or without the need for external energy input. To focus a sound of wavelength $\lambda$, and the lens positioned as shown in Figure 3.1, a mathematical formula (Appendix A) can be formed for determining $r_n$, the $n^{th}$ radius of the lens, represented by the blue arrows in Figure 2.3. Constructive superposition occurs when:

$$\frac{\lambda\,(4n-1)}{4} < \text{Path Difference} < \frac{\lambda\,(4n+1)}{4} \qquad (2.1)$$

$$r_n = \sqrt{\frac{\lambda(2n-1)(-\lambda+8L+2n\lambda)\big(16D(4D-\lambda+4L+2n\lambda)+\lambda^2+8L\lambda(2n-1)+4n\lambda^2(n-1)\big)}{512D(2D-\lambda+4L+2n\lambda)+64\lambda^2+512L(2L-\lambda+2n\lambda)+256n\lambda^2(n-1)}} \tag{2.2}$$

Using equation 2.2, radii up to $r_9$ were calculated, and a digital design was produced (Appendix B). A laser cutter produced lenses made of various materials, thicknesses, and sizes (Figure 2.4). There were no measurable differences ($\pm 0.5$ mm) between the design and the laser cut lenses.

Figure 2.4: Laser cut lenses

# 3 Method

Each lens was suspended in the middle of a large room (5 m $\times$10 m) to minimise the effects of reflections. The experiment was set up as shown in Figure 3.1, where the distance from the source to the lens $D$, the distance from the lens to the microphone $L$, and the frequency and amplitude of the sound could all be varied.

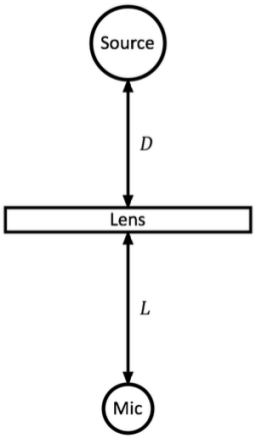


Figure 3.1: Setup

Logitech Z150 speakers (source) were used to play sounds with frequencies from 500 Hz to 12 kHz at 500 Hz intervals (sample audio file is available). Using a MOVO PM10 microphone, and an analytical program, Audacity 2.1.2, five second audio clips were recorded with and without various barriers. The amplification or attenuation ($A$) was calculated using equation 3.1.

$$A = I_{\text{final}} - I_{\text{original}} \text{ (all in dB)} \tag{3.1}$$

MATLAB R2016a in combination with k-wave 1.0.1 was used to run simulations (Appendix C) to predict the amplification at any point (Figure 3.2). Results were compared with the data collected. All tabulated variables apart from ambient temperature were varied individually to visualise the effect of each variable on the amplification and attenuation at different points in space.

| Variable | Value | Comments |
|---|---|---|
| Ambient temperature | $(15 \pm 2)$ °C | Speed of sound is $(340 \pm 1)$ m s$^{-1}$ |
| $D$ - distance source to lens | $(20.0 \pm 0.5)$ cm | Measured from front of speaker |
| $L$ - distance lens to microphone | $(20.0 \pm 0.5)$ cm | Measured to front of microphone |
| $f$ - frequency of sound | 10 kHz | Wavelength $(3.40 \pm 0.05)$ cm |
| Thickness of lens | 6 mm | |
| Number of hollow rings on lens | 5 | |
| Material of lens | Wood | Medium Density Fibreboard 700 kg m$^{-3}$ |

Table 3.1: Controlled variables and default values for independent variables

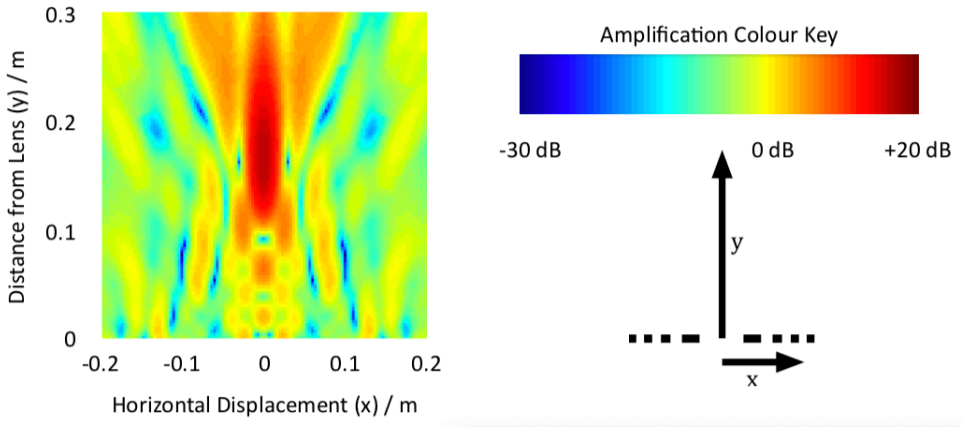


Figure 3.2: Visualising amplification simulation

# 4 Results

A visual overview of the effects of varying various parameters is provided in Figure 4.1, which uses the same amplification colour key as Figure 3.2

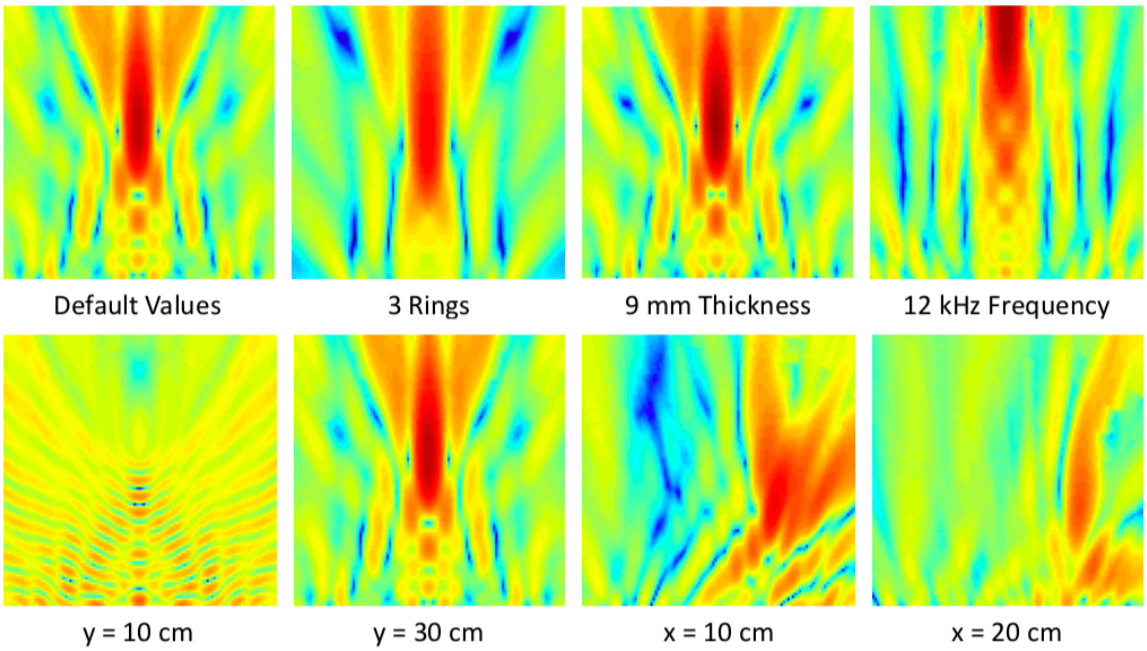


Figure 4.1: Visualisation of effects of varying parameters

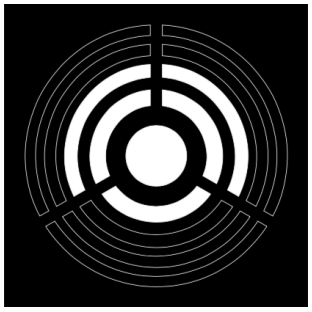

Figure 4.2: 2.67 Rings

The number of rings was varied by filling holes using the laser cut pieces. Figure 4.2 has 2.67 holes and by definition, 0 holes is a solid piece of material between the microphone and the speaker. A quantitative analysis of the number of rings vs amplification of 10 kHz at 20 cm is shown in Figure 4.3.

Further experiments were carried out to vary frequency (Figure 4.4), the position of the microphone (Figure 4.5), the material of the lens (Table 4.1) and the thickness of the lens (Table 4.2).

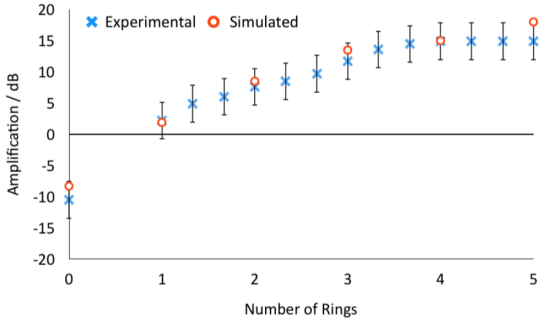


Figure 4.3: Number of rings vs amplification

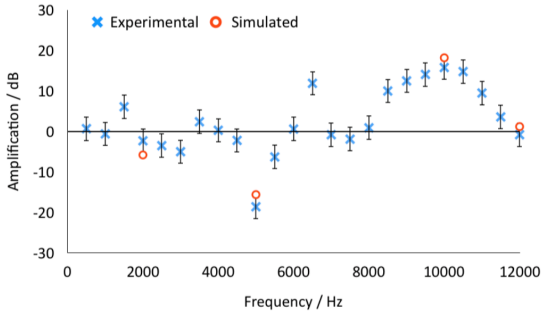


Figure 4.4: Frequency vs amplification

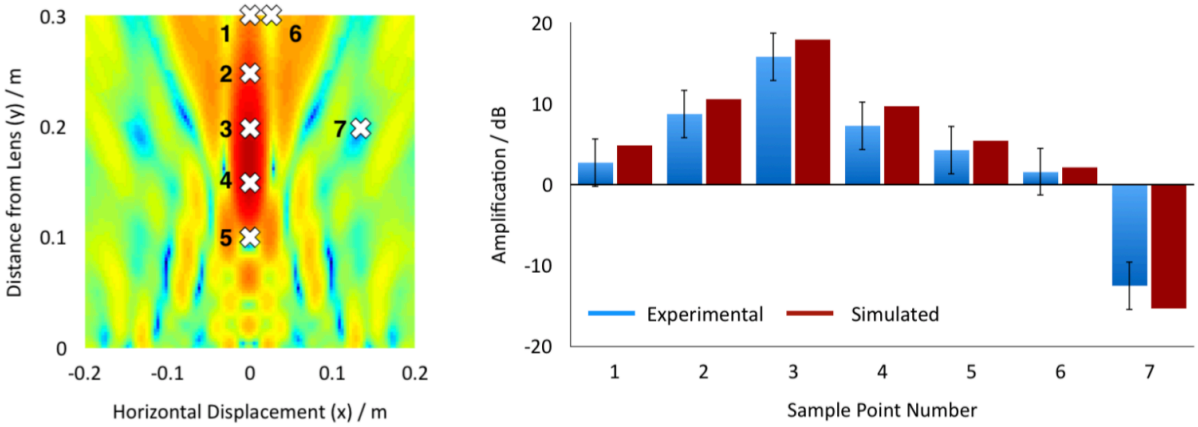


Figure 4.5: Microphone positions

| **Material** | $v_{\mathbf{sound}}$ / $\mathrm{m\,s^{-1}}$ | $\rho$/$\mathrm{kg\,m^{-3}}$ | **Z** / $\mathrm{kg\,m^{-2}\,s^{-1}}$ | $A_{\mathbf{Exp.}}$ / dB | $A_{\mathbf{Sim.}}$ / dB |
|---|---|---|---|---|---|
| Wood (MDF) | 3500 | 2500 | 8.75 | 15.8 ±2.8 | 18.0 |
| Acrylic Plastic | 2500 | 1000 | 2.50 | 10.3 ±3.1 | 13.2 |

Table 4.1: Lens material vs amplification

| **Thickness** / mm | $A_{\mathbf{Experimental}}$ / dB | $A_{\mathbf{Simulated}}$ / dB |
|---|---|---|
| 6 | 12.8 ±3.5 | 16.3 |
| 9 | 15.8 ±2.7 | 18.0 |

Table 4.2: Lens thickness vs amplification

# 5 Discussion

As expected, increasing the number of open rings (Figure 4.3) increases the amplification of sound from one or more rings, up to approximately 4 rings, from which point there appears to be no significant increase in amplification. Since sound waves reaching points of large $r$ are of small amplitudes due to attenuation in the air, and the diffracted waves' amplitudes are small at large angles, increasing the number of rings does not necessarily lead to large increases in amplification.

Increasing the frequency (Figure 4.4) changes the wavelength as they are related by the formula $v = f\lambda$. Since the superposition of waves is dependent on the wavelength, changing the frequency, and consequently the wavelength of the sound, alters the nature of the interference at a point in space, and some frequencies such as 10 kHz are amplified by over 10 dB while other frequencies such as 5 kHz are attenuated by 15 dB. Using the same lens in other media such as water, in which the speed of sound is $1500\,\mathrm{m\,s^{-1}}$, is also possible, but the frequencies of amplification and attenuation are altered.

The lens material (Table 4.1) also has an effect on the amplification. Intensity of reflected sound when transitioning between two media is determined by equation 5.1.

$$I_r = I_0 \frac{(Z_2 - Z_1)^2}{(Z_2 + Z_1)^2} \tag{5.1}$$

where $I_0$ is the incident intensity, $I_r$ is the reflected intensity and $Z_1$ and $Z_2$ are the acoustic impedance values for the two media. Using materials which have a large difference in acoustic impedance with air ($Z = 429\,\mathrm{kg\,m^{-2}\,s^{-1}}$) led to increased reflection, or decreased transmission through the blocked areas (Figure 4.2, black areas) which provide destructive components to the resultant wave.

Similarly, increasing the thickness of the lens (Table 4.2) increases the amplification at the focal point. This is predicted by Stoke's law of sound attenuation:

$$I = I_0 e^{-\mu x} \tag{5.2}$$

where $I_0$ is the incident intensity, $I$ is the transmitted intensity, $\mu$ is the attenuation coefficient of the material (which is frequency dependent), and $x$ is the distance travelled through the medium. This means that by increasing the thickness of the lens (increasing $x$), the transmitted sound intensity decreases, again through the blocked areas.

The main source of error in these experiments was the microphone, which had a measurement uncertainty of $\pm 3$ dB, and for small amplification values, led to a percentage error of just over 100 %. Use of a more expensive microphone would decrease this uncertainty, however, the strong correlation between currently obtained data and the computer simulations suggests that this is unnecessary. A further source of error is in the positioning of the microphone. As illustrated in Figure 3.2, a small change in position can lead to a large amplification difference. Again, more precise and accurate positioning systems could have been used, but are not strictly required.

Many difficulties were faced during the experimental phase of this project. Initially, a different microphone was used which led to resonant frequencies due to the length of the sensor emerging as data points, and so a much shorter and smaller microphone was used. Due to the experiment being carried out at home, reflections of sounds were inevitable, but its effects were minimised by using carpeted floors. To obtain more accurate results, an anechoic chamber can be used, which would further reduce reflections and external noise contributions.

# 6 Practical Uses

A simple application of this phenomenon is a targeted alarm clock: given the approximate distance from the target persons ear to the lens, a sound of the correct frequency can be played so that it is focused only for that person. This would allow others to remain undisturbed while successfully waking up the target. A video demonstration of this is available here: `https://youtu.be/X_WyB6UbMV4`.

On a larger scale, the same principles can be used to reduce noise pollution in residential areas. Road traffic has an approximate frequency range of 700 - 1300 Hz [4], and houses can be built in areas of large attenuation using larger scale Fresnel Zone Plates designed for this frequency. The most common solution to noise pollution currently is to build wooden or concrete walls which provide an average attenuation of 15 dB [5][6]. These 5 cm thick plywood barriers cost approximately $1000 per m [7], while a similar attenuation can be created by simply cutting 6 mm plywood into lenses costing just $200 per m, with further possible cost savings by recycling the cut wood.

# 7 Evaluation

The accuracy of producing the lens is high: on a 40 cm $\times$40 cm board, there was no measurable deviation from the digital design ($\pm$0.5 mm) which is approximately at most a 0.1% deviation. The biggest sources of error are in the microphone and positioning systems, and the effects of these have been discussed above.

The assumptions that are made for superposition and diffraction to occur are applicable in real life for sounds up to 150 dB, but since 120 dB is the approximate threshold of pain for humans, non-linear acoustics was not considered in this report.

Simulating acoustics is a very computationally intense process, taking an average computer over 15 hours to simulate one experiment. This time was reduced to just over 10 minutes by using the McMillan computing cluster at Princeton University. For commercial research and development, this process may be one of the most time consuming phases, but will inevitably become less significant with the further increase of computational power.

As seen in Figure 4.4, the amplification is highly frequency dependent, and so a lens could "fail" at its intended function. For example, a lens designed to attenuate sounds of 5 kHz would amplify sounds of 10 kHz which may not be desirable. However, since the human ear is most responsive in the range 500 Hz to 5000 Hz [8], this can be accounted for in the design and simulation phases.

# 8 Limitations and Further Work

Currently, the proposed design for reducing noise pollution from traffic has only been tested with a computer simulation. Although the simulations on a smaller scale do fit well with practical data collected supporting the validity of this simulation, practical testing must be carried out to truly validate the design. The costs of materials and the physical limitation of the laser cu@er used, restricted experimental testing to a 40 cm $\times$40 cm lens.

# 9 Acknowledgements

I would like to thank Gavin Jennings, Gareth Hodges, and Kent Hogan for their insightful discussions. Special thanks to Byung Cheol Cho who provided access to the McMillan computing cluster at Princeton University.

# Appendices

## A Derivation


Constructive interference occurs for $\frac{\lambda(4n-1)}{4} < d + l - D - L < \frac{\lambda(4n+1)}{4}$

Destructive interference occurs everywhere else. This means a boundary occurs every $\frac{(2n-1)\lambda}{4}$, giving $d + l - D - L = \frac{n\lambda}{2} - \frac{\lambda}{4}$

Using the Pythagorean theorem, $d = \sqrt{D^2 + r_n^2}$ and $l = \sqrt{L^2 + r_n^2}$

From substitution: $\sqrt{D^2 + r_n^2} + \sqrt{L^2 + r_n^2} - D - L = \frac{n\lambda}{2} - \frac{\lambda}{4}$

Or rearranging for $r_n$ gives

$$r_n = \sqrt{\frac{\lambda(2n-1)(-\lambda+8L+2n\lambda)\left(16D(4D-\lambda+4L+2n\lambda)+\lambda^2+8L\lambda(2n-1)+4n\lambda^2(n-1)\right)}{512D(2D-\lambda+4L+2n\lambda)+64\lambda^2+512L(2L-\lambda+2n\lambda)+256n\lambda^2(n-1)}}$$

## B Sample Lens Design

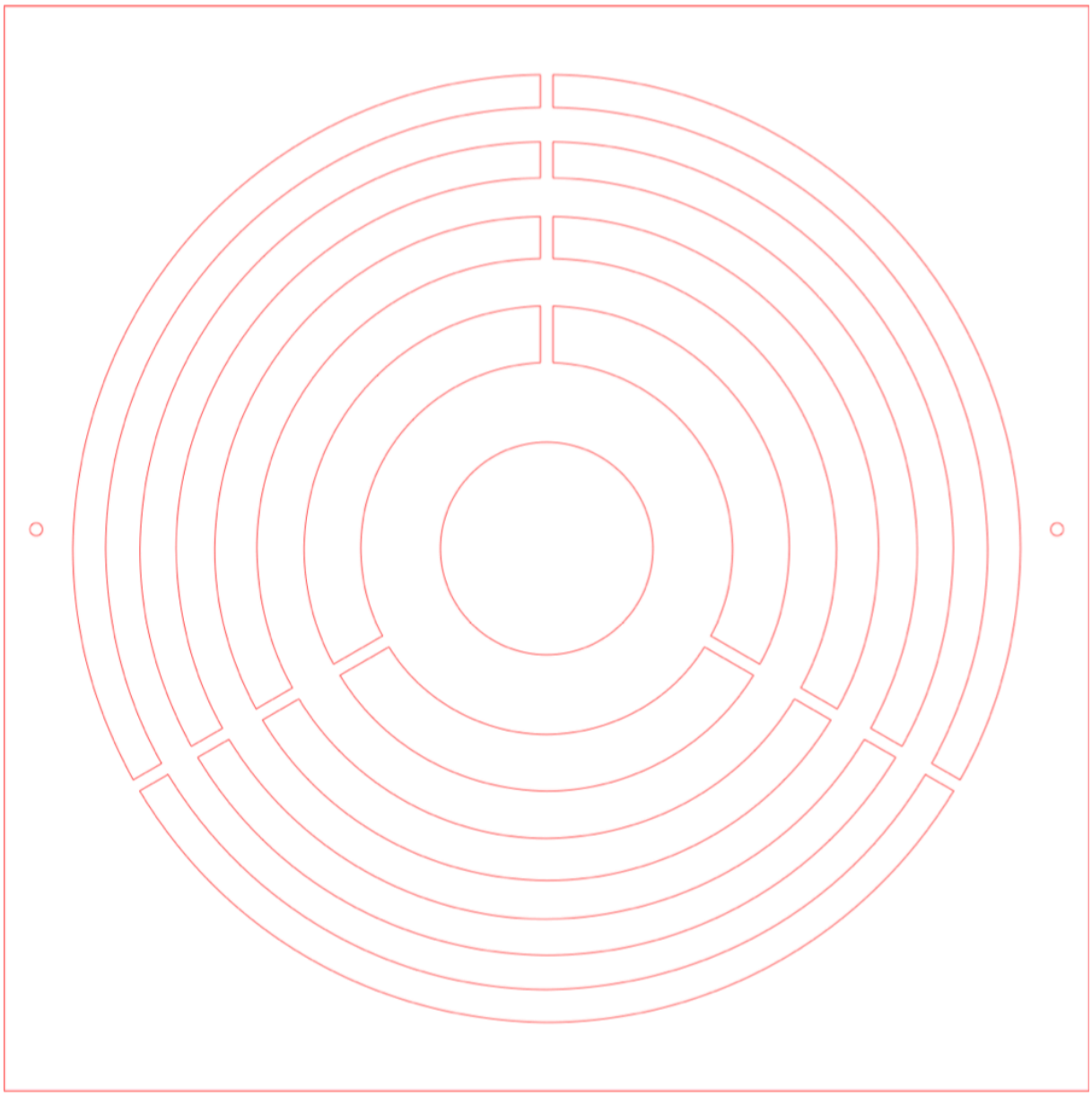

## C Sample Code

```
% Requires k-wave library

freq = 5e3;                         % Source frequency [Hz]
source_to_slit = 0.2;               % Distance from source to lens [m
    ]

Nx = 256;                           % Number of grid points in x (
    longitudinal) direction
Ny = 160;                           % Number of grid points in y
    direction
Nz = 160;                           % Number of grid points in z
    direction
dx = source_to_slit * 4 / Nx;       % Grid point spacing in the x
    direction [m]
dy = dx;                            % Grid point spacing in the y
    direction [m]
dz = dx;                            % Grid point spacing in the z
    direction [m]

kgrid = makeGrid(Nx, dx, Ny, dy, Nz, dz);

% Properties of medium (air)
c0 = 343;                           % Speed of sound [m/s]
rho0 = 1.225;                       % Density [kg/m
medium.sound_speed = c0 * ones(Nx, Ny, Nz); % [m/s]
medium.density = rho0 * ones(Nx, Ny, Nz);   % [kg/m
medium.alpha_power = 1.5;
medium.alpha_coeff = (3e-3) / (freq/1e6)medium.alpha_power; % [dB
    /(MHzy cm)]

t_end = dx * Nx / c0;               % [s]
CFL = 0.02;
[kgrid.t_array, dt] = makeTime(kgrid, medium.sound_speed, CFL,
    t_end);
Nt = length(kgrid.t_array);

% Point Source
source.p_mask = zeros(Nx, Ny, Nz);
source.p_mask(end - Nx / 4, Ny / 2, Nz / 2) = 1;

% Time varying sinusoidal wave
source_freq = freq;                 % [Hz]
source_mag = 10;                    % [Pa]
source.p = source_mags * sin(2 * pi * source_freq * kgrid.t_array
    );
source.p = filterTimeSeries(kgrid, medium, source.p);
sensor.mask = ones(Nx, Ny, Nz);

% Barrier/Lens
barrier_thickness = 6;              % Lens thickness [mm]
```

```
grid_thickness = round(barrier_thickness / 1e3 / dx); % [m]
radii_mm = [41.63, 72.87, 95.05, 113.6, 130.09, 145.22, 159.38,
   172.8, 185.65]; % [mm]
radii_grids = round(radii_mm / 1e3 / dy);
barrier_mask = zeros(Nx, Ny, Nz);
disc1 = reshape(makeDisc(Ny, Nz, Ny / 2, Nz / 2, radii_grids(1)),
    1, Ny, Nz);
disc2 = reshape(makeDisc(Ny, Nz, Ny / 2, Nz / 2, radii_grids(3))
   & makeDisc(Ny, Nz, Ny / 2, Nz / 2, radii_grids(2)), 1, Ny, Nz);
disc3 = reshape(makeDisc(Ny, Nz, Ny / 2, Nz / 2, radii_grids(5))
   & makeDisc(Ny, Nz, Ny / 2, Nz / 2, radii_grids(4)), 1, Ny, Nz);
disc4 = reshape(makeDisc(Ny, Nz, Ny / 2, Nz / 2, radii_grids(7))
   & makeDisc(Ny, Nz, Ny / 2, Nz / 2, radii_grids(6)), 1, Ny, Nz);
disc5 = reshape(makeDisc(Ny, Nz, Ny / 2, Nz / 2, radii_grids(9))
   & makeDisc(Ny, Nz, Ny / 2, Nz / 2, radii_grids(8)), 1, Ny, Nz);
template = disc1 | disc2 | disc3 | disc4 | disc5;
barrier_mask(Nx / 2:(Nx / 2 + grid_thickness - 1), :, :) = repmat
   (template, grid_thickness, 1, 1);

% Control (no barrier)
if control
    barrier_sound_speed = 3500;
    barrier_density = 700;
    medium.sound_speed(barrier_mask == 1) = barrier_sound_speed;
    medium.density(barrier_mask == 1) = barrier_density;
end

% Acoustic parameters to record
sensor.record = {'p_final', 'p_max_all', 'p_rms'};
sensor.record_start_index = floor(0.8 * Nt);

input_args = {'DisplayMask', barrier_mask | source.p_mask, '
   DataCast', 'single'};
sensor_data = kspaceFirstOrder3D(kgrid, medium, source, sensor,
   input_args{:});

if control
    save('3D_request_05_withbarrier.mat', '-v7.3');
else
    save('3D_request_05_nobarrier.mat', '-v7.3');
end
```

## D Frequency Response of Microphone (Experimental)

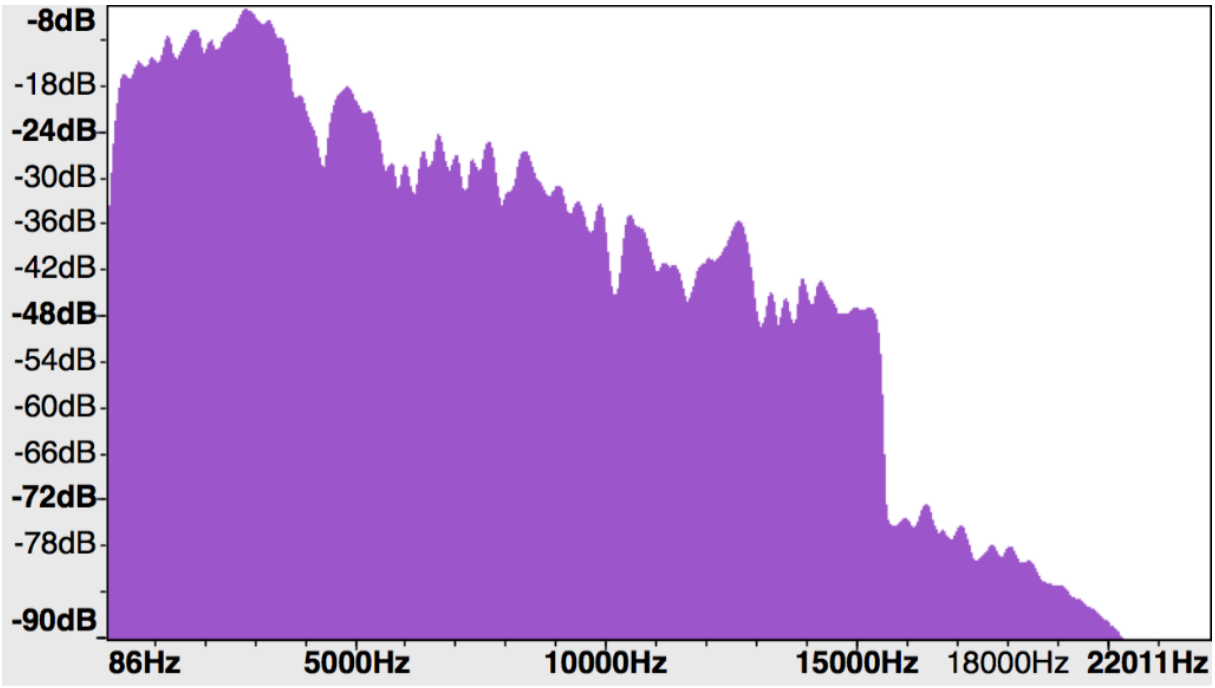

## References

[1] Y. Li, G. Yu, B. Liang, X. Zou, G. Li, S. Cheng, and J. Cheng, "Three-dimensional Ultrathin Planar Lenses by Acoustic Metamaterials," *Scientific Reports*, vol. 4, no. 1, May 2015. [Online]. Available: http://www.nature.com/articles/srep06830

[2] D. C. Calvo, A. L. Thangawng, M. Nicholas, and C. N. Layman, "Thin Fresnel zone plate lenses for focusing underwater sound," *Applied Physics Letters*, vol. 107, no. 1, p. 014103, Jul. 2015. [Online]. Available: http://aip.scitation.org/doi/10.1063/1.4926607

[3] "Fresnel Lens of Sound." [Online]. Available: http://www.ncsm.city.nagoya.jp/cgi-bin/en/exhibiton_guide/exhibit.cgi?id=S406

[4] U. Sandberg, "The multi-coincidence peak around 1000 hz in tyre/road noise spectra," *Euronoise Naples 2003*, vol. 498, 01 2003.

[5] "Design of wood highway sound barriers." [Online]. Available: http://woodcenter.org/docs/fplrp596.pdf

[6] "Sound Levels." [Online]. Available: https://acoustics.nzta.govt.nz/sound-levels

[7] "State highway noise barrier design guide." [Online]. Available: https://www.nzta.govt.nz/resources/state-highway-noise-barrier-design-guide/

[8] S. Rawashdeh, "Frequency Response of the Ear." [Online]. Available: https://au.mathworks.com/matlabcentral/fileexchange/16101